Isotopic scaling of heavy projectile residues from the collisions of 25 MeV/nucleon ^{86}Kr with ^{124}Sn, ^{112}Sn and ^{64}Ni, ^{58}Ni

G. A. Souliotis, D. V. Shetty, M. Veselsky,* G. Chubarian, L. Trache, A. Keksis, E. Martin, and S. J. Yennello

Cyclotron Institute, Texas A&M University, College Station, Texas 77843, USA

The scaling of the yields of heavy projectile residues from the reactions of 25 MeV/nucleon ^{86}Kr projectiles with ^{124}Sn, ^{112}Sn and ^{64}Ni, ^{58}Ni targets is studied. Isotopically resolved yield distributions of projectile fragments in the range $Z=10–36$ from these reaction pairs were measured with the MARS recoil separator in the angular range $2.7°–5.4°$. For these deep inelastic collisions, the velocities of the residues, monotonically decreasing with Z down to $Z \simeq 26–28$, are employed to characterize the excitation energy. The ratios $R_{21}(N,Z)$ of the yields of a given fragment (N,Z) from each pair of systems are found to exhibit isotopic scaling (isoscaling), namely, an exponential dependence on the fragment atomic number Z and neutron number N. The isoscaling is found to occur in the residue Z range corresponding to the maximum observed excitation energies. The corresponding isoscaling parameters are $\alpha=0.43$ and $\beta=-0.50$ for the Kr+Sn system and $\alpha=0.27$ and $\beta=-0.34$ for the Kr+Ni system. For the Kr+Sn system, for which the experimental angular acceptance range lies inside the grazing angle, isoscaling was found to occur for $Z \leq 26$ and $N \leq 34$. For heavier fragments from Kr+Sn, the parameters vary monotonically, α decreasing with Z and β increasing with N. This variation is found to be related to the evolution towards isospin equilibration and, as such, it can serve as a tracer of the N/Z equilibration process. The present heavy-residue data extend the observation of isotopic scaling from the intermediate mass fragment region to the heavy-residue region. Interestingly, such high-resolution mass spectrometric data can provide important information on the role of isospin and isospin equilibration in peripheral and midperipheral collisions, complementary to that accessible from modern large-acceptance multidetector devices.

I. INTRODUCTION

The isotopic composition of nuclear reaction products contains important information on the role of the isospin on the reaction dynamics [1]. Recently, increased interest in the N/Z degree of freedom and its equilibration [2–5], as well as in the isospin asymmetry dependent terms of the nuclear equation of state [6,7], has motivated detailed measurements of the isotopic distributions of fragments with $Z \geq 2$ [8–11]. Isotopically resolved data in the region $Z=2–8$ have revealed systematic trends, but their N/Z properties are unavoidably affected by the decay of the excited primary fragments. It has recently been shown [12] that isospin effects can be investigated by comparing the yields of fragments from two similar reactions that differ only in the isospin asymmetry. In this case, the effect of sequential decay of primary fragments can be bypassed to a large extent. It has been revealed that for statistical fragment production mechanism(s), if two reactions occurring at the same temperature have different isospin asymmetry, the ratio $R_{21}(N,Z)$ of the yields of a given fragment (N,Z) obtained from the two reactions 2 and 1 exhibits an exponential dependence on N and Z of the form

$$R_{21}(N,Z) = C \exp(\alpha N + \beta Z),$$

where α and β are the scaling parameters and C is an overall

normalization constant. This scaling behavior is called isotopic scaling or isoscaling [12], and has been observed in a variety of reactions under the conditions of statistical emission and equal temperature [13–16]. (If the temperatures are different, a generalized isoscaling can be obtained with appropriate temperature corrections [17].) The isoscaling parameters α and β are shown to contain information on the early stages of fragment formation (before sequential deexcitation). It remains a matter of further investigation to what extent they may provide information on the type and the details of the reaction mechanism(s).

Up to the present, the isoscaling phenomenon has been systematically investigated with isotopically resolved fragments not heavier than $Z=8$. It would be interesting to investigate the behavior of heavier fragments up to the region of heavy residues. Heavy residues are known to comprise a large fraction of the reaction cross section at the intermediate energy regime [18]. However, efficient collection and complete characterization of the residues in terms of their atomic number Z, mass number A, ionic charge state q, and velocity requires the use of a magnetic spectrometer. At this point, it should be noted that the scaling behavior of heavy fragment yields from light particle induced reactions at relativistic energies on separated Sn targets has been recently reported [19]. In Ref. [19], the fragment yields were measured with radiochemical techniques. With mass spectrometric techniques, however, apart from isotopically resolved yields, the velocities of the fragments can be obtained with high resolution and can provide information on the excitation energy of the primary fragments.

---

*On leave from the Institute of Physics of the Slovak Academy of Sciences, Bratislava, Slovakia.

In the present work, isotopic scaling is investigated for fragments obtained in high-resolution mass spectrometric studies of projectile fragments from the reactions of 25 MeV/nucleon ^{86}Kr with ^{124,112}Sn and ^{64,58}Ni targets. Yield ratios of fragments with $Z=10-36$ were obtained and isotopic scaling was investigated. Using the velocities of the residues, the excitation energy of the hot primary fragments was characterized. Finally, the values of the isoscaling parameters were used to provide isospin information on the hot emitting sources. The paper is organized as follows. In Sec. II, a brief description of the experimental apparatus, the measurements, and the data analysis is given. In Sec. III, after examining the average velocity and N/Z characteristics of the fragments, the isotopic scaling of the fragment yields is studied in detail. Finally, conclusions from the present study are summarized in Sec. IV.

II. EXPERIMENTAL METHODS AND DATA ANALYSIS

The present study was performed at the Cyclotron Institute of Texas A&M University. A 25 MeV/nucleon^{86}Kr^{22+} beam from the K500 superconducting cyclotron, with a typical current of ~ 1 pnA, interacted with isotopically enriched targets of ^{124}Sn, ^{112}Sn (2 mg/cm^2), and ^{64}Ni, ^{58}Ni (4 mg/cm^2). The reaction products were analyzed with the MARS spectrometer [20] offering an angular acceptance of 9 msr and momentum acceptance of 4%. The primary beam struck the target at 4.0° relative to the optical axis of the spectrometer. The direct beam was collected inside the target chamber on a square Faraday cup lying outside of the angular acceptance of the spectrometer. Fragments were accepted in the polar angular range 2.7°–5.4°. This angular range lies inside the grazing angle of 6.5° of the Kr+Sn reactions and mostly outside the grazing angle of 3.5° of the Kr+Ni reactions at 25 MeV/nucleon [21]. It should be noted that the spectrometer angle setting was chosen to optimize the production of very neutron-rich fragments from the Kr+Sn systems whose detailed study is reported elsewhere [22]. An Al foil (1 mg/cm^2) was used to reset to equilibrium the ionic charge states of the projectile fragments. MARS optics [20] provides one intermediate dispersive image and a final achromatic image (focal plane). At the focal plane, the fragments were collected in a 5×5 cm^2 two-element $(\Delta E, E)$ Si detector telescope. The ΔE detector was a position-sensitive Si strip detector of 110 μm thickness, whereas the E detector was a single-element Si detector of 950 μm. Time of flight was measured between two PPACs (parallel plate avalanche counters) positioned at the dispersive image and at the focal plane, respectively, and separated by a distance of 13.2 m. The PPAC at the dispersive image was also X-Y position sensitive and used to record the position of the fragments. The horizontal position, along with nuclear magnetic resonance measurements of the field of the MARS first dipole, was used to determine the magnetic rigidity $B\rho$ of the particles. The reaction products were characterized by an event-by-event measurement of energy loss, residual energy, time of flight, and magnetic rigidity. The response of the spectrometer/detector system to ions of known atomic number Z, mass number A, ionic charge q, and velocity was

calibrated using a low intensity ^{86}Kr primary beam and other beams at 25 MeV/nucleon.

The determination of the atomic number Z was based on the energy loss of the particles in the ΔE detector [23] and their velocity. The ionic charge q of the particles entering MARS was obtained from the total energy $E_{tot} = \Delta E + E$, the velocity, and the magnetic rigidity. The measurements of Z and q had resolutions of 0.5 and 0.4 units [full width at half maximum (FWHM)], respectively. Since the ionic charge must be an integer, we assigned integer values of q for each event by putting windows ($\Delta q = 0.4$) on each peak of the q spectrum. Using the magnetic rigidity and velocity measurement, the mass-to-charge A/q ratio of each ion was obtained with a resolution of 0.3%. Combining the q determination with the A/q measurement, the mass A was obtained as: $A = q_{int} A/q$ (q_{int} is the integer ionic charge) with a resolution (FWHM) of $0.6A$ units. Combination and normalization of the data at the various magnetic rigidity settings of the spectrometer (in the range 1.3–2.0 T m), summation over all ionic charge states (with corrections applied for missing charge states [24]), and, finally, normalization for beam current and target thickness provided fragment yield distributions with respect to Z, A, and velocity. Further details of the analysis procedure can be found in Ref. [25] and in previous work with heavier beams [26–28]. The yield distributions, summed over velocities, were used to obtain the yield ratios $R_{21}(N,Z) = Y_2(N,Z)/Y_1(N,Z)$ employed in the present isotopic scaling studies.

III. RESULTS AND DISCUSSION

Before embarking on the discussion of the yield ratios and scaling, we will first examine the velocity and N/Z characteristics of the reaction products. It is well established that reactions between massive nuclei around the Fermi energy [18] proceed via a deep inelastic transfer mechanism involving substantial nucleon exchange [29–32]. This mechanism is responsible for the creation of highly excited primary fragments that deexcite to produce the observed fragments. To obtain information about the excitation energy of the primary fragments from the present reactions, we will first examine the correlation of the measured velocity with the atomic number. Figure 1 presents the average velocities of the fragments as a function of Z. Closed symbols correspond to the reactions with the neutron-rich targets and open symbols to those with the neutron-poor targets. In this figure, we observe that for fragments close to the projectile, the velocities are slightly below that of the projectile, corresponding to very peripheral, low-excitation-energy events. A monotonic decrease of velocity with decreasing Z is observed, indicative of lower impact parameters, higher momentum transfers, and thus higher excitation energies.

For the ^{86}Kr+^{124,112}Sn reactions [Fig. 1(a)], the descending velocity-Z correlation continues down to $Z \sim 28$; for lower Z's, the velocity appears to increase with decreasing Z. The appearance of a minimum velocity for $Z \sim 28$ can be understood by assuming that these residues originate from primary fragments with a maximum observed excitation energy. Fragments with Z near the projectile down to $Z \sim 28$
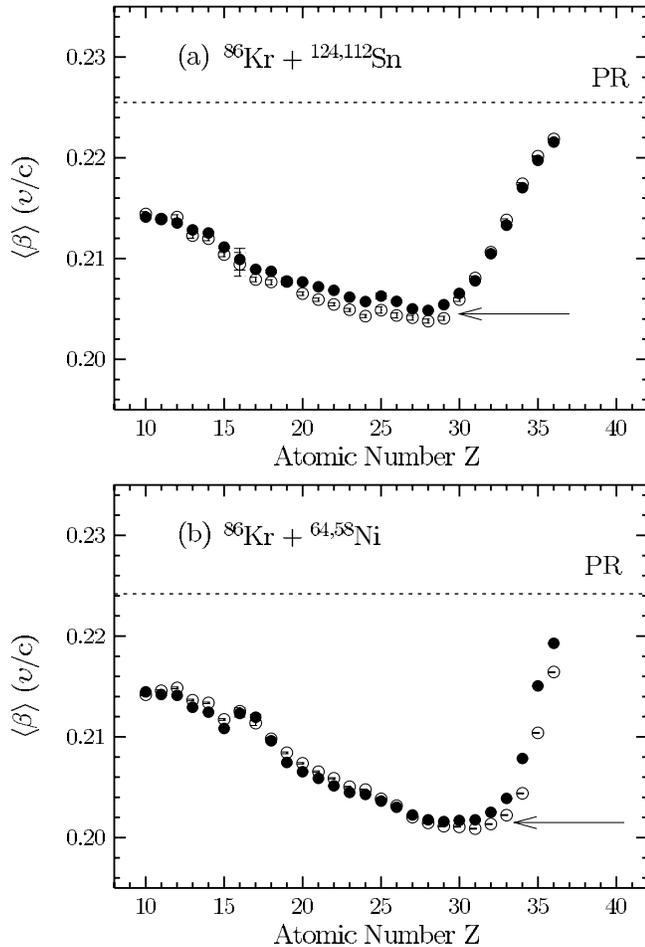
FIG. 1. Average velocity vs atomic number Z correlations for projectile residues from the reactions of (a) ^{86}Kr (25 MeV/nucleon) with ^{124}Sn and ^{112}Sn, and (b) ^{86}Kr (25 MeV/nucleon) with ^{64}Ni and ^{58}Ni. Full circles represent the data with the neutron-rich targets ^{124}Sn and ^{64}Ni, and open circles those with the neutron-poor targets ^{112}Sn and ^{58}Ni. The dashed line (marked "PR") gives the velocity of the projectile, whereas the arrows indicate the minimum average residue velocities observed (see text).

originate from evaporative type of deexcitation which does not modify, on average, the emission direction of the residues. Thus, the residue velocities can provide information on the excitation energy. Residues with lower Z arise, as we will discuss below, from primary fragments undergoing cluster emission and/or multifragmentation and the velocity of the inclusively measured fragments is not monotonically correlated with the excitation energy, the mass A, or the atomic number Z. For the ^{86}Kr$+^{64,58}$Ni reactions, a similar behavior is observed. However, the decreasing velocity-Z correlation is observed only down to $Z\sim32$. It should be pointed out that fragments from this reaction were measured mostly outside the grazing angle, so that they correspond to more damped collisions, in such a way that the final residues receive a larger recoil during the deexcitation stage and appear within this angular range. For $Z\sim30$–32, we observe a minimum velocity and for lower Z's an increase of the velocity with decreasing Z. The average velocities from the reactions with the neutron-rich targets are, within the experimental un-

certainties, almost the same as the corresponding velocities from the reactions with the neutron-deficient targets for both pairs of systems. For both reactions, the ascending part of the velocity vs Z correlation for the lower part of the Z range is primarily due to the combined effect of angle and magnetic rigidity selection. The forward angle range $(2.7°–5.4°)$ selects either the forward or the backward kinematical solution in the moving frame of the quasiprojectile undergoing cluster emission or multifragmentation, whereas the magnetic rigidity range $(1.3–2.0 \, \mathrm{T\,m})$ subsequently selects the forward solution.

Employing the observed minimum velocities for the Kr$+$Sn and Kr$+$Ni reactions and, furthermore, applying two-body kinematics and equal division of excitation energy (which is a reasonable assumption for nearly symmetric systems at this energy regime [32,33]), we can estimate an average excitation energy per nucleon for the hot quasiprojectile fragments of $E^*/A=2.2\pm0.1$ MeV for both Kr$+$Sn and Kr$+$Ni systems. Using the Fermi gas relationship $E^* =(A/K)T^2$, with T the tempretature and K the inverse level density parameter, taken as $K=13$ MeV [34], we can estimate the temperature of Kr-like quasiprojectiles as $T=5.3\pm0.2$ MeV for both systems. This average temperature is in the range typical for reaction processes near the multifragmentation threshold [10,34]. In addition, this temperature is rather close to the limiting temperature of excited nuclei of $A\sim90$ according to the recent systematics of Natowitz *et al.* [35]. Since these excitation energy estimates are average values obtained from average residue velocities, we may assume that surviving residues with even lower velocities originating from even higher excitation energies are produced in the present measurements. However, due to the inclusive nature of the measurements and the velocity fluctuations due to evaporation, we cannot select residue source velocities lower than those indicated by the average velocities.

In Fig. 2, we present the average N/Z values for each Z for the Kr$+$Sn reactions (upper panel) and Kr$+$Ni reactions (lower panel). In the figures, the N/Z values from the reactions involving the neutron-rich targets are shown with full circles and those involving the neutron-poor targets with open circles. The horizontal dashed line (marked "PR") represents the N/Z of the ^{86}Kr projectile. The thin solid line gives the line of β stability (marked "SL") obtained from the relation $Z_\beta=A/(1.98+0.0155A^{2/3})$ [36]. Finally, the dotted line represents the evaporation attractor line (EAL) [37] corresponding to the locus of fragment yields produced by evaporation of neutrons and charged particles from highly excited nuclei close to stability. (The statistical deexcitation code GEMINI was used to obtain the position of the EAL [38].)

For the Kr$+$Sn reactions, we observe that the average N/Z of the fragments close to the projectile rapidly decreases with deceasing Z down to approximately $Z=26$–28. For lower Z, the average N/Z appears to be grossly constant with a possible dip around $Z=15$. The Z value below which the average N/Z of the fragments is roughly constant coincides with the Z value corresponding to the minimum residue velocity, as previously discussed in relation to Fig. 1. As ex-
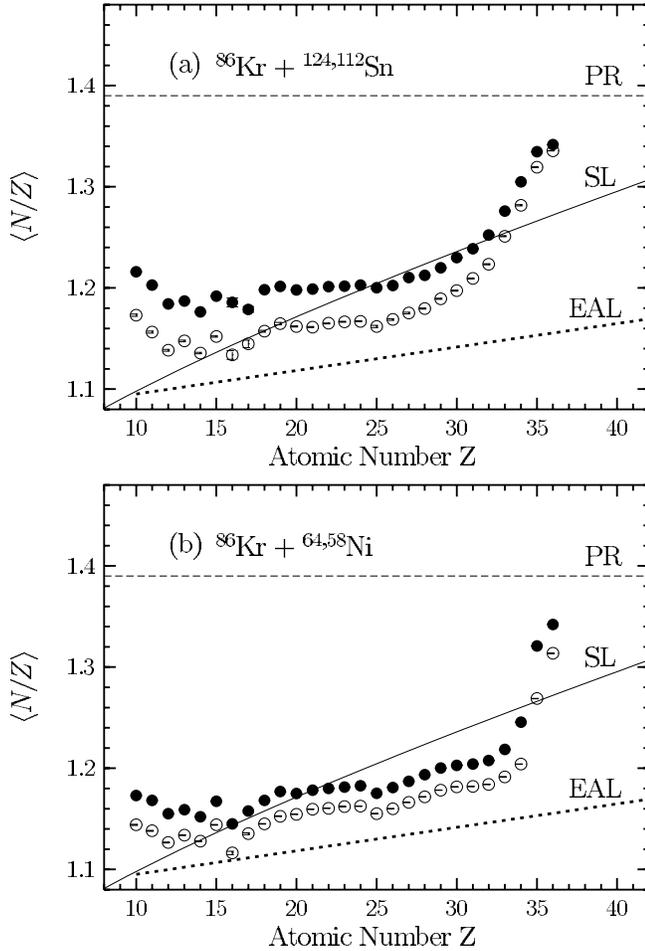
FIG. 2. Average N/Z vs atomic number Z correlations for projectile residues from the reactions of (a) ^{86}Kr (25 MeV/nucleon) with ^{124}Sn and ^{112}Sn, and (b) ^{86}Kr (25 MeV/nucleon) with ^{64}Ni and ^{58}Ni. Full circles represent the data with the neutron-rich targets ^{124}Sn and ^{64}Ni, and open circles those with the neutron-poor targets ^{112}Sn and ^{58}Ni. The dashed line (marked "PR") gives the N/Z of the projectile, the solid line (marked "SL") is the line of stability, and the dotted line (marked "EAL") is the evaporation attractor line [37] (see text).

pected, the N/Z of the fragments from the reactions with the neutron-rich ^{124}Sn are larger than those from the reactions with the neutron-poor ^{112}Sn target. This difference appears to be largest below $Z\sim26$, namely, close to the onset of cluster emission and/or multifragmention. In this region, the fragment N/Z deviates from its course towards or beyond (to the neutron-poor side of) the stability line and appears to be roughly constant. This feature of multifragmentation of very neutron-rich heavy systems may be exploited in the production of neutron-rich rare isotopes and it will be the topic of a subsequent study.

For the Kr+Ni reactions, similar observations can be made in Fig. 2(b). For these reactions, the rapid decrease of N/Z is observed down to $Z=32$, corresponding to the Z with the minimum average velocity [Fig. 1(b)]. Below $Z=32$, the N/Z shows a slight decrease and then, below $Z=26$ it becomes roughly constant (again with a dip at $Z\sim15$, as for Kr+Sn).

Having examined the excitation energy and N/Z characteristics of the measured residue data, we turn our discussion to the scaling properties of the fragment yields. According to the equilibrium limit of the grand-canonical ensemble, a thermally equilibrated system undergoing statistical decay can be characterized by a primary fragment yield with neutron number N, and proton number Z of the form [39,40]

$$Y(N,Z)=F(N,Z)\exp[B(N,Z)/T]\exp(N\mu_n/T+Z\mu_p/T),$$
(1)

where the factor $F(N,Z)$ represents contributions due to the secondary decay from particle stable and unstable states to the final ground state; μ_n and μ_p are the neutron and proton chemical potentials; $B(N,Z)$ is the ground state binding energy of the corresponding fragment, and T is the temperature.

A direct comparison of the observed yield distributions with Eq. (1) is not possible due to the distortions introduced by the sequential decay of the primary fragments. However, it has been shown [12] that the ratio of the yields $Y_2(N,Z)/Y_1(N,Z)$ of a given fragment (N,Z) from two different reacting systems, having similar masses and excitation energies but differing only in N/Z, can be used to obtain information about the excited primary fragments. If the main difference between the two systems 2 and 1 is the isospin, then the binding energy terms in Eq. (1) cancel out in the ratio $Y_2(N,Z)/Y_1(N,Z)$. Furthermore, if one assumes that the influence of the secondary decay on the yields is similar for the two reactions, then a relation of the form

$$R_{21}(N,Z)=Y_2(N,Z)/Y_1(N,Z)=C\exp(\alpha N+\beta Z) \quad (2)$$

can be obtained with $\alpha=\Delta\mu_n/T$ and $\beta=\Delta\mu_p/T$, with $\Delta\mu_n$ and $\Delta\mu_p$ being the differences in the neutron and the proton chemical potentials of the fragmenting systems. C is an overall normalization constant. The ratio $R_{21}(N,Z)$ is insensitive to the sequential decay and thus it can provide information on the decaying excited primary fragments.

From the present data, we construct the yield ratio $R_{21}(N,Z)$ using the convention that index 2 refers to the more neutron-rich system and index 1 to the less neutron-rich one. Figure 3 shows the yield ratios $R_{21}(N,Z)$ as a function of fragment neutron number N for selected isotopes (top panel) and proton number Z for selected isotones (bottom panel) for the Kr+Sn reactions. The different isotopes and isotones considered are shown by alternating filled and open symbols for clarity. In Fig. 4, the corresponding ratios for the Kr+Ni reactions are shown.

As it can be seen in the top panels of Figs. 3 and 4, the ratios for each element Z exhibit a remarkable exponential behavior. For each element, an exponential function of the form $C\exp(\alpha N)$ was fitted to the data and also shown in Fig. 4 for the selected elements. In the semilog representation, the lines for each element are nearly parallel up to $Z\sim28$ for Kr+Sn and up to $Z\sim34$ for Kr+Ni (in the latter case exhausting the whole range of observed fragments). For heavier fragments from the Kr+Sn systems, the fits to the data show gradual decrease in the slopes with increasing Z of the fragments. An analogous behavior is observed in the lower panels of Figs. 3 and 4, where the ratio $R_{21}(N,Z)$ is
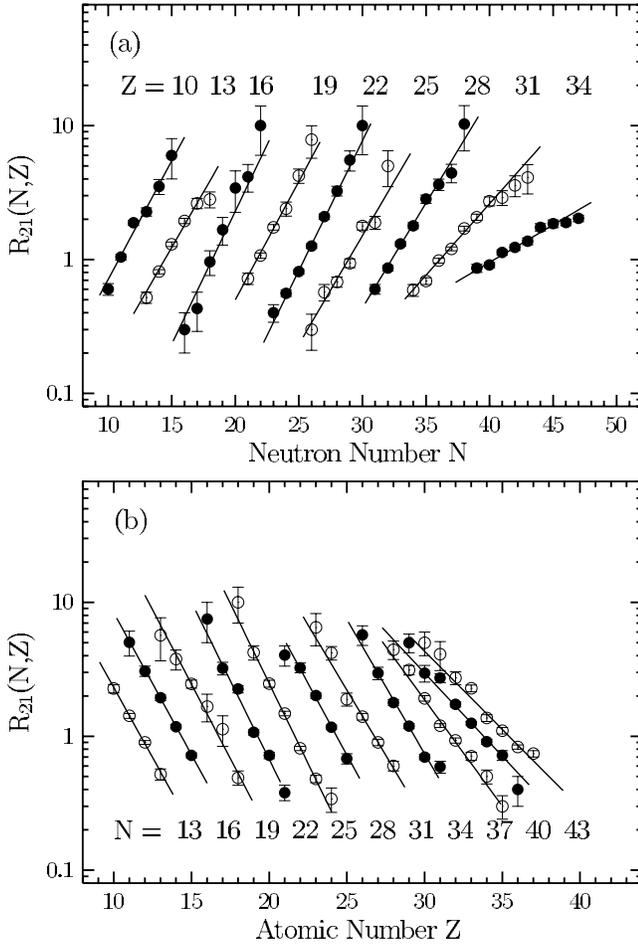
FIG. 3. Yield ratios $R_{21}(N,Z)=Y_2(N,Z)/Y_1(N,Z)$ of projectile residues from the reactions of ^{86}Kr (25 MeV/nucleon) with ^{124,112}Sn (a) with respect to N for the Z's indicated, and (b) with respect to Z for the N's indicated. The data are given by alternating filled and open circles, whereas the lines are exponential fits (see text).
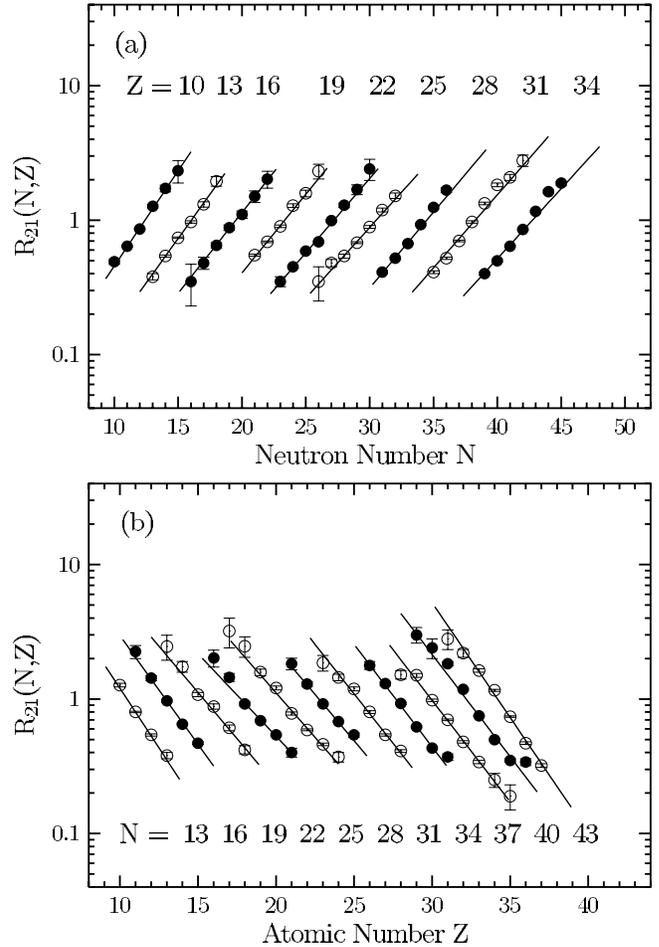

FIG. 4. Yield ratios $R_{21}(N,Z)=Y_2(N,Z)/Y_1(N,Z)$ of projectile residues from the reactions of ^{86}Kr (25 MeV/nucleon) with ^{64,58}Ni (a) with respect to N for the Z's indicated, and (b) with respect to Z for the N's indicated. The data are given by alternating filled and open circles, whereas the lines are exponential fits (see text).

plotted as a function of Z for various isotones. The solid lines correspond to exponential fits using the expression $C \exp(\beta Z)$. The ratios $R_{21}(N,Z)$ appear to lie along straight lines with nearly similar negative slopes β, for all isotones up to $N \sim 34$ for Kr+Sn and $N \sim 44$ for Kr+Ni (again, in the latter case covering the whole fragment range). For larger N from Kr+Sn, the slopes β increase with increasing N of the fragments. The positive slopes in the upper panels of Figs. 3 and 4 indicate that neutron-rich fragments are more efficiently produced, as expected, from the more neutron-rich systems. Similarly, the negative slopes in the bottom panels of these figures indicate that proton-rich fragments are more efficiently produced from the more proton-rich systems.

In Fig. 5, we present the slope parameters α (upper panel) and β (lower panel) of the exponential fits (obtained as described for Figs. 3 and 4) as a function of Z and N. For the Kr+Sn reactions, the slope parameter α is roughly constant with an average value of 0.43 in the range $Z=10–26$ and then decreases for $Z>26$. Similarly, the parameter β appears to be nearly constant at an average value of -0.50 up to $N \sim 34$ and rise for $N>34$. Consequently, for the Kr+Sn sys-

tems under the present experimental conditions, isoscaling (as defined in Ref. [12]) holds up to $Z \sim 26$ and $N \sim 34$. This fragment range corresponds to primary events with the maximum observed excitation energy of 2.2 MeV/nucleon and temperature of 5.3 MeV, as estimated previously. For the Kr+Ni reactions, the slope parameter α appears to be constant in the whole range $Z=10–36$ at an average value $\alpha =0.27$. Similarly, the parameter β remains constant at an average value of -0.34 in the whole N range. In the case of the Kr+Ni systems under the present experimental conditions (observation outside the grazing angle), isoscaling holds in the whole range of observed fragments, corresponding to primary events having on average excitation energy of 2.2 MeV/nucleon and temperature of 5.3 MeV. The near constancy of the isoscaling parameters α and β (except for near-projectile fragments for the Kr+Sn system) corroborates the statistical nature of the fragment production under the excitation energy and temperature values extracted from the minimum observed residue velocities. In general, the extracted isoscaling parameters α and β are in agreement with the corresponding values reported in the literature (e.g., Refs. [12,15]).
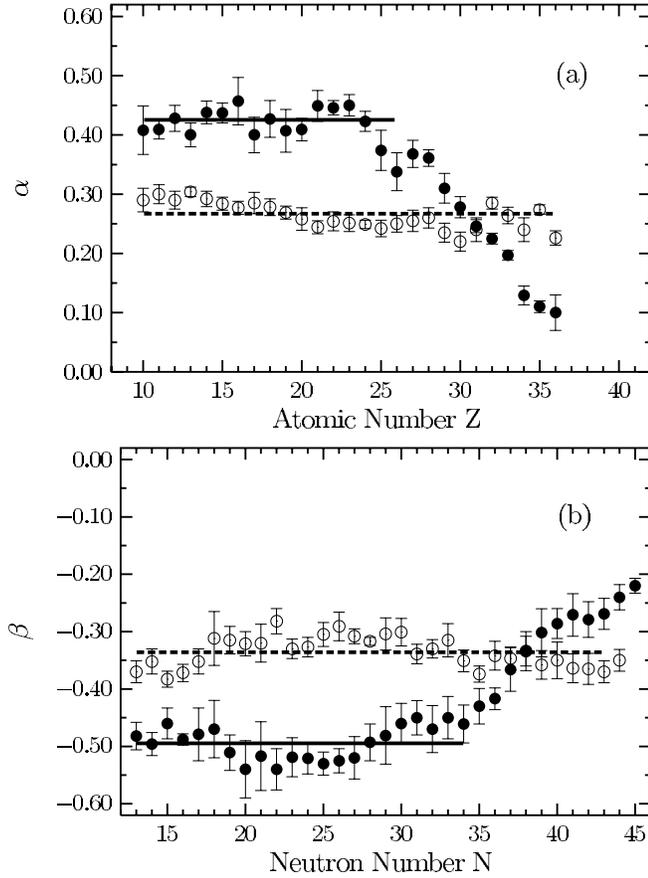
FIG. 5. (a) Isoscaling parameter α as a function of Z for projectile residues from the reactions ^{86}Kr (25 MeV/nucleon) + ^{124,112}Sn (closed circles) and ^{86}Kr (25 MeV/nucleon) + ^{64,58}Ni (open circles). The straight lines are constant value fits for each system (see text). (b) Isoscaling parameter β as a function of N for ^{86}Kr (25 MeV/nucleon) + ^{124,112}Sn (closed circles) and ^{86}Kr (25 MeV/nucleon) + ^{64,58}Ni (open circles). The straight lines are again constant value fits for each system.

In the following discussion, we will use the isoscaling parameters herein obtained to extract information about the hot primary fragments. As we have already mentioned, the parameters α and β are related to the differences in the neutron and proton chemical potentials of the corresponding pri-mary fragmenting systems via the relations $\alpha = \Delta\mu_n / T$ and $\beta = \Delta\mu_p / T$. Using the average values of the parameters α and β and the estimated temperatures, we can obtain the differences in the chemical potentials, as summarized in Table I. As seen in the table, these values are close (apart from a difference in sign) [10,15] to the corresponding differences in the neutron and proton separation energies, as obtained from mass tables [41]. The corresponding values for the protons appear to be remarkably close (Table I).

It has been shown [14,15] that the isoscaling parameter α is directly related to the coefficient C_{sym} of the symmetry-energy term of the nuclear binding energy. The following relation has been obtained both in the framework of the grand-canonical limit of the statistical multifragmentation model [15] and in the expanding-emitting source model [14]:

$$\alpha = 4\frac{C_{sym}}{T}\left[\left(\frac{Z_1}{A_1}\right)^2 - \left(\frac{Z_2}{A_2}\right)^2\right], \qquad (3)$$

where Z_1, A_1, and Z_2, A_2 refer to the fragmenting quasiprojectiles from reactions 1 and 2, respectively. Using this relation, the extracted values of α and T for the fragments corresponding to multifragmentation events and assuming N/Z equilibration (see following discussion and Fig. 6), we get for C_{sym} the values of 27.2 for Kr + Sn and 23.1 for Kr + Ni (Table I). These estimates of the symmetry-energy coefficient are in reasonable agreement with the standard value $C_{sym} = 25$ MeV [15].

In principle, Eq. (3) can serve as the basis for determining C_{sym} for expanded multifragmenting nuclei [14] thus probing the density dependence of the symmetry-energy term of the nuclear equation of state. However, such experimental determination requires systematic isotopically resolved yield measurements with good excitation energy characterization. With the present spectrometric approach, in order to avoid the uncertainties in excitation energy division, as well as in N/Z equilibration, such measurements may be performed for symmetric pairs differing in isospin (e.g., ^{64}Ni + ^{64}Ni and ^{58}Ni + ^{58}Ni or ^{124}Sn + ^{124}Sn and ^{112}Sn + ^{112}Sn). In such cases, the excitation energies (and temperatures) can be obtained from the residue velocities and the average N/Z of the quasiprojectiles can be taken as that of the reacting system.

TABLE I. Excitation energy E^*/A (MeV/nucleon), temperature T(MeV), isoscaling parameters α and β, differences in neutron and proton chemical potentials $\Delta\mu_n$(MeV) and $\Delta\mu_p$(MeV), differences in neutron and proton separation energies ΔS_n(MeV) and ΔS_p(MeV), and extracted symmetry-energy coefficient C_{sym} (MeV) for the systems ^{86}Kr (25 MeV/nucleon) + ^{124,112}Sn and ^{86}Kr (25 MeV/nucleon) + ^{64,58}Ni (see text). Parentheses give estimated errors (one standard deviation).

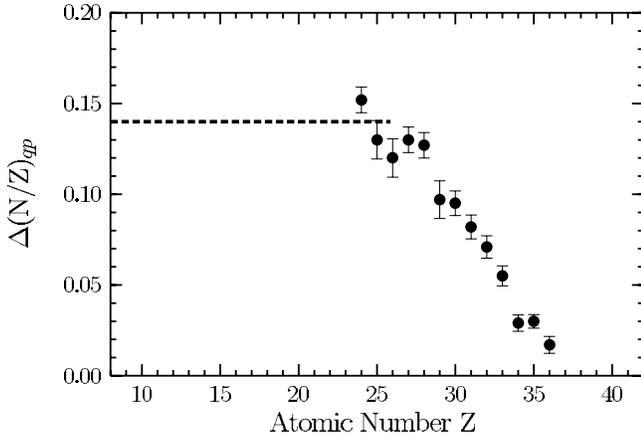| Reaction	E^*/A	T	α	β	$\Delta\mu_n$	$\Delta\mu_p$	ΔS_n	ΔS_p	C_{sym}
Kr + Sn	2.2	5.3	0.43	−0.51	2.28	−2.65	−1.44	2.23	27.2
	(0.1)	(0.2)	(0.03)	(0.03)	(0.18)	(0.19)			(2.2)
Kr + Ni	2.2	5.3	0.27	−0.34	1.43	−1.80	−2.75	1.77	23.1
	(0.1)	(0.2)	(0.02)	(0.02)	(0.11)	(0.13)			(1.9)

FIG. 6. Difference in N/Z of the fragmenting quasiprojectiles [obtained using Eq. (4)] as a function of Z for projectile residues from the reactions ^{86}Kr (25 MeV/nucleon)$+\,^{124,112}$Sn (closed circles). The dashed line gives the N/Z difference of isospin-equilibrated fragmenting quasiprojectiles.

Finally, we will employ Eq. (3) to provide an interpretation of the variation of the isoscaling parameter α with Z for the Kr+Sn reactions and relate this variation to the isospin-equilibration process. After some manipulation, from Eq. (3) we obtain

$$\alpha = 8\frac{C_{sym}}{T}\left(\frac{Z}{A}\right)^3_{ave}\Delta\left(\frac{N}{Z}\right)_{qp} \tag{4}$$

where $(Z/A)_{ave}$ is the average Z/A of the quasiprojectiles, taken to be the average Z/A of the composite systems ^{86}Kr $+\,^{124}$Sn and ^{86}Kr$+\,^{112}$Sn, and $\Delta(N/Z)_{qp}$ expresses the N/Z difference of fragmenting quasiprojectiles corresponding to a given value of fragment Z, isoscaling parameter α, and temperature T. Assuming that fragments are produced at normal density, using $C_{sym}=25$ MeV [15], the α values obtained from the isoscaling fits, and the temperatures determined from excitation energies (obtained from residue velocities), we can determine the value of $\Delta(N/Z)_{qp}$ as a function of the observed fragment Z, as shown in Fig. 6. In this figure, the horizontal line expresses the N/Z difference of fragmenting quasiprojectiles under the condition of isospin equilibration.

The essentially monotonic increase of $\Delta(N/Z)_{qp}$ with decreasing Z can be understood as follows. Fragments close to the projectile are produced in very peripheral collisions in which a small number of nucleons is exchanged and thus, the N/Z difference of the fragmenting quasiprojectiles from ^{86}Kr$+\,^{124}$Sn and ^{86}Kr$+\,^{112}$Sn is small. Fragments progressively further from the projectile originate from collisions with larger projectile-target overlap in which a large number of nucleons is exchanged. In such cases, the N/Z difference of the fragmenting quasiprojectiles is progressively larger, eventually approaching, for the present energy regime, the N/Z difference corresponding to isospin equilibration. Consequently, the variation of the isoscaling parameter α with Z (and, equivalently, β with N) for near-projectile residues is a result of the variation in the N/Z of the fragmenting quasiprojectiles, directly related to the course towards isospin

equilibration. As such, the parameter α along with temperature (excitation energy) determination can be used as a sensitive probe to study the isospin-equilibration process in collisions of isospin asymmetric massive nuclei at intermediate energies. A detailed account on this approach is reported elsewhere [42].

The present high-resolution mass spectrometric data provided information on the isoscaling properties of heavy projectile fragments and, subsequently, information on the de-excitation of hot primary fragments, as well as, the degree of N/Z equilibration. Along these lines, it should be noted that with the same spectrometric techniques, we recently obtained information on the details of the deexcitation mechanisms of heavy fragments and the onset of multifragmentation in the reaction of ^{124}Sn (25 MeV/nucleon) with ^{27}Al [43]. These recent efforts in the Fermi energy regime (following earlier work with heavier beams [26,27]), along with similar studies at relativistic energies (e.g., Refs. [44,45] and references therein), indicate that detailed isotopic and kinematic investigation of heavy residues provides essential information on the reaction mechanisms and the details of the deexcitation processes that can complement the results of full-acceptance devices. As a possible next step, combination of high-resolution mass separators with advanced large-acceptance multidetector arrays may allow novel and exciting studies of reaction dynamics, furthermore taking advantage of the availability of rare isotope beams.

IV. SUMMARY AND CONCLUSIONS

In summary, the isotopic scaling of heavy projectile residues from the interaction of 25 MeV/nucleon ^{86}Kr projectiles with ^{124}Sn, ^{112}Sn and ^{64}Ni, ^{58}Ni targets has been studied. Isotopically resolved yield distributions of projectile fragments in the range $Z=10-36$ from the above reaction pairs were measured with the MARS recoil separator in the angular range $2.7°-5.4°$. For these deep inelastic collisions, the velocities of the residues, monotonically decreasing with Z down to $Z\sim26-28$, are employed to characterize the excitation energy. The yield ratios $R_{21}(N,Z)$ for each pair of systems are found to exhibit isoscaling, namely, an exponential dependence on the fragment atomic number Z and neutron number N. The isoscaling is found to occur in the residue Z range corresponding to the maximum observed excitation energies. The corresponding isoscaling parameters are $\alpha=0.43$ and $\beta=-0.50$ for the Kr+Sn system and $\alpha=0.27$ and $\beta=-0.34$ for the Kr+Ni system. For the Kr+Sn system, for which the experimental angular acceptance range lies inside the grazing angle, isoscaling was found to occur for $Z\leqslant26$ and $N\leqslant34$. The values of the isoscaling parameters are used to extract the neutron and proton chemical potentials, as well as to obtain an estimate of the symmetry-energy coefficient of highly excited primary fragments. For heavy fragments from Kr+Sn, the isoscaling behavior breaks down and the parameters are found to vary monotonically, α decreasing with Z and β increasing with N. This variation of the isoscaling parameters for near-projectile

residues is found to be related to the evolution towards iso-spin equilibration and, as such, can serve as a tracer of N/Z equilibration. The present isotopically resolved heavy-residue data demonstrate the occurrence of isotopic scaling from the intermediate mass fragment region to the heavy-residue region. Such high-resolution mass spectrometric data have the potential to provide important information on the role of isospin and isospin equilibration in peripheral and midperipheral collisions, complementary to that accessible from advanced large-acceptance multidetector devices.

[1] *Isospin Physics in Heavy Ion Collisions at Intermediate Energies*, edited by B.-A. Li and W. Schroeder (Nova Science, New York, 2001).

[2] S.J. Yennello *et al.*, Phys. Lett. B **321**, 15 (1994).

[3] F. Rami *et al.*, Phys. Rev. Lett. **84**, 1120 (2000).

[4] B.-A. Li and S.J. Yennello, Phys. Rev. C **52**, 1746 (1995).

[5] H. Johnston *et al.*, Phys. Lett. B **371**, 186 (1996).

[6] B.-A. Li, C.M. Ko, and W. Bauer, Int. J. Mod. Phys. E **7**, 147 (1998).

[7] H. Müller and B.D. Serot, Phys. Rev. C **52**, 2072 (1995).

[8] H.S. Xu *et al.*, Phys. Rev. Lett. **85**, 716 (2000).

[9] R. Laforest *et al.*, Phys. Rev. C **59**, 2567 (1999).

[10] M. Veselsky *et al.*, Phys. Lett. B **497**, 1 (2001).

[11] E. Ramakrishnan *et al.*, Phys. Rev. C **57**, 1803 (1998).

[12] M.B. Tsang *et al.*, Phys. Rev. Lett. **86**, 5023 (2001).

[13] M.B. Tsang *et al.*, Phys. Rev. C **64**, 041603 (2001).

[14] M.B. Tsang *et al.*, Phys. Rev. C **64**, 054615 (2001).

[15] A.S. Botvina, O.V. Lozhkin, and W. Trautmann, Phys. Rev. C **65**, 044610 (2002).

[16] D. V. Shetty *et al.*, Phys. Rev. C (to be published).

[17] M.B. Tsang *et al.*, Phys. Rev. C **66**, 044618 (2002).

[18] H. Fuchs and K. Möhring, Rep. Prog. Phys. **57**, 231 (1994).

[19] J. Adam *et al.*, nucl-ex/0302032.

[20] R.E. Tribble, R.H. Burch, and C.A. Gagliardi, Nucl. Instrum. Methods Phys. Res. A **285**, 441 (1989).

[21] W.W. Wilcke *et al.*, At. Data Nucl. Data Tables **25**, 389 (1980).

[22] G.A. Souliotis *et al.*, Phys. Rev. Lett. **91**, 022701 (2003).

[23] F. Hubert, R. Bimbot, and H. Gauvin, At. Data Nucl. Data Tables **46**, 1 (1990).

[24] A. Leon *et al.*, At. Data Nucl. Data Tables **69**, 217 (1998).

[25] G.A. Souliotis *et al.*, Phys. Lett. B **543**, 163 (2002).

[26] G.A. Souliotis *et al.*, Nucl. Phys. **A705**, 279 (2002).

[27] G.A. Souliotis *et al.*, Phys. Rev. C **57**, 3129 (1998).

[28] G.A. Souliotis *et al.*, Phys. Rev. C **55**, 2146 (1997).

[29] M. Veselsky, Nucl. Phys. **A705**, 193 (2002).

[30] J.F. LeColley *et al.*, Phys. Lett. B **325**, 317 (1994).

[31] M. Morjean *et al.*, Nucl. Phys. **A591**, 371 (1995).

[32] M. Veselsky *et al.*, Phys. Rev. C **62**, 064613 (2000).

[33] H. Madani *et al.*, Phys. Rev. C **54**, 1291 (1996).

[34] J.B. Natowitz *et al.*, Phys. Rev. C **65**, 034618 (2002).

[35] J.B. Natowitz *et al.*, Phys. Rev. C **66**, 031601 (2002).

[36] *Physics of Nuclei and Particles*, edited by P. Marmier and E. Sheldon (Academic Press, New York, 1970), Vol. 1, p. 15.

[37] R. Charity, Phys. Rev. C **58**, 1073 (1998).

[38] R. Charity, Nucl. Phys. **A483**, 391 (1988).

[39] S. Albergo *et al.*, Nuovo Cimento Soc. Ital. Fis., A **89**, 1 (1985).

[40] J. Randrup and S.E. Koonin, Nucl. Phys. **A356**, 223 (1981).

[41] P. Moller, J.R. Nix, and K.L. Kratz, At. Data Nucl. Data Tables **66**, 131 (1997).

[42] G.A. Souliotis, M. Veselsky, and S.J. Yennello, nucl-ex/0305027, Phys. Lett. B (to be published).

[43] M. Veselsky *et al.*, Nucl. Phys. **A724**, 431 (2003).

[44] K.-H. Schmidt, M.V. Ricciardi, A.S. Botvina, and T. Enqvist, Nucl. Phys. **A710**, 157 (2002).

[45] M.V. Ricciardi *et al.*, Phys. Rev. Lett. **90**, 212302 (2003).